Fish and Shellfish Immunology 88 (2019) 578–586

Contents lists available at ScienceDirect

Fish and Shellfish Immunology

journal homepage: www.elsevier.com/locate/fsi

Full length article

In vivo multivesicular bodies and their exosomes in the absorptive cells of the zebrafish (*Danio Rerio*) gut

Xuebing Bai[a], Yanna Guo[a], Yonghong Shi[a], Jinxing Lin[b], Imran Tarique[a], Xindong Wang[a], Waseem Ali Vistro[a], Yufei Huang[a], Hong Chen[a], Abdul Haseeb[a], Ping Yang[a], Qiusheng Chen[a,*]

[a] *MOE Joint International Research Laboratory of Animal Health and Food Safety, College of Veterinary Medicine, Nanjing Agricultural University, Nanjing, Jiangsu Province, 210095, China*

[b] *Shanghai Laboratory Animal Research Center, Shanghai, 201203, China*

ARTICLE INFO

Keywords:
Multivesicular bodies (MVBs)
In vivo exosomes
Absorptive cell
Gut mucosa immunity
Zebrafish

ABSTRACT

Intercellular communication of gut epithelial cells is critical to gut mucosal homeostasis. Exosomes are important intercellular mediators in communication between cell to cell. Although many literature focus on the immunologic roles in the gut by the exosomes, the biological process of exosomes in the absorptive cells remains unknown. Uncovering the distribution, classification and formation process of multivesicular bodies (MVBs) and their exosomes in the absorptive cells of the zebrafish gut, is urgently needed to establish a platform for immunological research of fish gut exosomes. The expression levels of CD63 and TSG101 were different among the three segments of the gut, and they were enriched at the apex of the mid gut villi. The characteristics of MVBs and their exosomes in the absorptive cells were further revealed by transmission electron microscopy (TEM). Early endosomes (ee) were mainly present in the apical and basal cytoplasm of absorptive cells. Late endosomes (le) were mostly distributed with the supranuclear part of these cells. "Heterogeneous" MVBs were detected underlying the apical membranes of absorptive cells. Many exosomes with some MVB-like structures occurred in the lumen, indicating that the release process was mainly through apical secretion. Various MVBs with exosomes and the endosome-heterogeneous MVB-exosome complex existed widely in the mid gut absorptive cells, concluding that zebrafish as a potential model for in vivo MVBs and their exosomes research. All the results were summarized in a schematic diagram illustrating the morphological characteristics of gut MVBs and their exosomes in zebrafish.

1. Introduction

Exosomes are membrane-bound vesicles with a diameter of 30–150 nm, which has received much attention in the past few years due to their role in intercellular communication [1] and immunity related research through trafficking of a wide variety of proteins, lipids, mRNAs and microRNAs [2] to neighbouring cells or distant cells.

Exosomes are developed by the inward budding of the local membrane of late endosomes (le) during the maturation of multivesicular bodies (MVBs) and released when fuse of MVBs with the plasma membrane [3]. There are two mechanisms of exosome development. Exosomes can be formed in an endosomal sorting complexes required for transport (ESCRT)-dependent pathway, tumor susceptibility gene 101 (TSG101) is a member of the ESCRT-I complex and binds to ubiquitinated cargo proteins to promote the formation of exosomes [4,5]. Previous experimental data have proven that deletion of TSG101 results in a significant reduction in exosomes [6]. In addition, an ESCRT-independent pathway can also produce large amounts of exosomes, such as lysosomal associated membrane protein 3 (CD63), which is one of the tetraspanin family proteins is particularly enriched in the surface of exosomes and has been shown to be involved in endosomal sorting in melanocytes [7–10]. Hence, CD63 and TSG101 are commonly used as biomarkers for the study of MVBs and exosomes. Exosomes exist in biological body fluids [11] and are released by a variety of cells, including gut absorptive epithelial cells [12]. The gut epithelial cells have well-developed endocytosis and exocytosis [13,14]. Endocytosis can introduce cell membrane proteins and exogenous antigens into the cell, while exocytosis transports substances to the outside of the cell, which maintains the dynamic balance of the cell and the organism. Importantly, MVBs with protein sorting functions are important intermediaries between the two processes, and they are either transferred to lysosomes to be degraded or fused with the plasma membrane to

---

[*] Corresponding author. College of Veterinary Medicine, Nanjing Agricultural University, Nanjing, Jiangsu Province, 210095, China.
E-mail address: chenqsh305@njau.edu.cn (Q. Chen).

https://doi.org/10.1016/j.fsi.2019.03.030
Received 21 September 2018; Received in revised form 21 February 2019; Accepted 12 March 2019

release exosomes.

A wide range of physiological [15,16] and pathological [17–20] functions have been attributed to exosomes in the gut system, especially in the antigen presentation process between gut immune cells. Exosome pathways are essential for the maintenance of gut mucosal immunity homeostasis, including exosomes secreted by intestinal epithelium cells (IECs) infected with rotavirus that exerting inhibit regulatory T cells effects [18]. IECs infected with protozoan parasite *Cryptosporidium parvum* (*C. parvum*) release exosomes carrying antimicrobial factors to promote epithelial barrier function [20]. IECs secrete “tolerosomes” carrying luminal antigens to induce oral tolerance [21]. In addition, antigen presenting cells (APCs) with MVBs can exert immunity through exosomes, so we speculate that fish intestinal epithelial cells containing MVBs, like APCs cells, also have similar immune functions.

Zebrafish have a simple structure, transparent embryos, short growth cycle, prolific breeding, defined genetic background, and approximately 70% genetic conservation with humans [22]. It is also a well animal model to investigate various diseases [23]. The mucosa of the gut forms a vast interface between the immune cells of lamina propria and gut lumen microenvironment. It serves as a physical and immunological barrier, and it also plays a crucial role in defence against pathogenic bacteria and viruses. Dynamic balance among mucus layers, gut epithelial cells, and luminal contents is essential for the maintenance of gut homeostasis. Although the zebrafish gut structure has been well studied [24–27], it is largely unknown whether exosomes will be secreted by the gut of zebrafish.

In this study, we aimed to identify the characteristics of in vivo MVBs and their exosomes from absorptive cells in the zebrafish gut system. We studied the exosome secretion process of absorptive cells at the subcellular level. Our results provide the first in vivo insight into the release process of MVBs and their exosomes from zebrafish gut absorptive cells.

2. Materials and methods

2.1. Animals

Adult zebrafish come from the Shanghai Laboratory Animal Research Center and were maintained at a constant 28 °C, with continuous water circulation in the lab. All experiments were performed using wild type AB zebrafish (*Danio rerio*), aged six months (n = 200). Zebrafish were anaesthetized by MS-222 (150 mg/L) (A5040, Sigma, Saint Louis, Missouri, USA). All tasks were executed to minimize animal suffering and experiments were approved by the Experimental Animal Ethics Committee of Nanjing Agricultural Veterinary College (The approval ID is SYXK (SU) 2010–0005).

2.2. Tissue sampling

Whole zebrafish (n = 20) were embedded in paraffin wax to prepare tissue sections for light microscopy (HE, IHC, IF). Zebrafish (n = 180) were sacrificed, and the internal organs, including liver, spleen, gut, pancreas and gall bladder, were promptly removed as a whole to avoid damage to individual tissues. The other organs around the gut were dissected to obtain a clean gut sample that was separated into anterior, mid and posterior gut based on the anatomical structure. Samples of the three different segments were then prepared for RT-qPCR, WB and TEM protocols as described below.

2.3. Hematoxylin and eosin staining (H&E)

Samples prepared for paraffin sectioning were fixed in 10% neutral buffered formalin overnight. Samples were sectioned at a thickness of 7 μm by a microtome device (Leica, RM2245, Germany). In brief, after deparaffinization and hydration, slides were stained with hematoxylin for 1.5 min, rinsed with water for 5 min, then incubated in an alcohol gradient and stained in eosin for 3 s. Following dehydration through increasing alcohol concentrations and xylene washes, the section was sealed with neutral gum. Then, samples were observed with a light microscope (DP73, Olympus, Tokyo, Japan).

Table 1
Primer sequences used for RT-qPCR.

Target genes	Primer sense (5′-3′)	Primer antisense (5′-3′)
CD63	ATGGCTGTAGAAGGAGGAGC	GCCGTGTTGTGCAAAGAAAC
TSG101	ACTACTGTGGGTCCAAGTCG	CTGTGCTCTGTCCATCTCCT
β-actin	CCCTGAATCCCAAAGCCAAC	TCACACCATCACCAGAGTCC

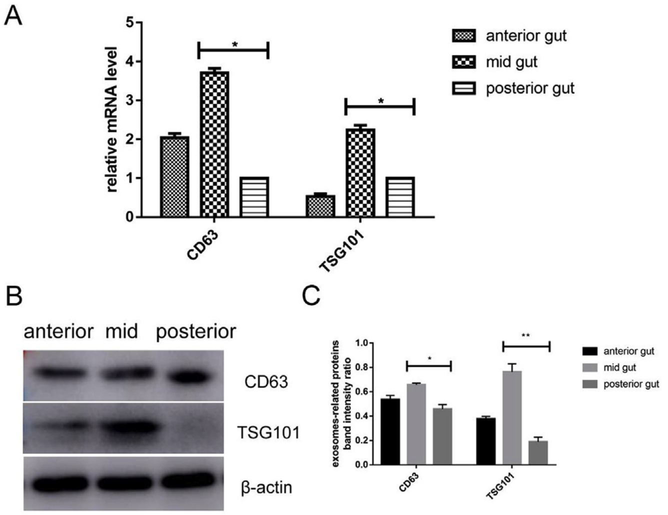

Fig. 1. The mRNA and protein levels of CD63 and TSG101 in the mid gut are higher than those in the anterior and posterior gut. (A) CD63 and TSG101 mRNA level in different gut detected by quantitative RT-PCR (RT-qPCR). (B) Western blot analysis of CD63 and TSG101 protein level in three segments of gut. The histogram represents the densitometric analysis of the immunoblots (*$P < 0.05$; *$P < 0.01$) compared to the posterior gut.

2.4. Real-time quantitative PCR (RT-qPCR)

Follow the manufacturer's instructions, total RNA was extracted from the gut (anterior, mid, posterior) using TRIzol reagent (Invitrogen, Carlsbad, CA, USA). Reverse transcription (HiScript®II 1st Strand cDNA Synthesis Kit, Vazyme) of the RNA was performed with the primers listed in Table 1. Two microliters of template RNA were reacted with SYBR Greeen master mix for a total volume of 20 μl (Vazyme). The thermal cycling conditions were 5 min at 95 °C, followed by 40 cycles of 10 s at 95 °C and 30 s at 60 °C using a LightCylcer SW 1.1 quantitative real-time PCR system.

2.5. Western blot analysis (WB)

β-actin (4970, Cell Signaling Technology, Beverly, MA, USA; 1:1000) served as the loading control for the WB analysis. Proteins were extracted from the zebrafish gut (anterior, mid, posterior) with ice-cold RIPA buffer (25 mM Tris/HCl (pH 7.6), 1% Nonidet-P40, 150 mM NaCl, 0.1% SDS, 1% sodium deoxycholate, and 0.05 mM PMSF) and sedimented for 10 min at 15,000 g, 4 °C. Then, the total protein concentration was determined with the BCA protein assay kit (Thermo Fisher Scientific, USA). The same amounts of protein (200 μg/lane) were resolved on a 10% SDS-PAGE gel, and then all proteins were transferred onto polyvinylidene di-fluoride (PVDF) (Millipore, Bedford, MA) membranes. The membranes were closed with 5% non-fat milk and incubated at 4 °C overnight with the primary antibody (CD63 and

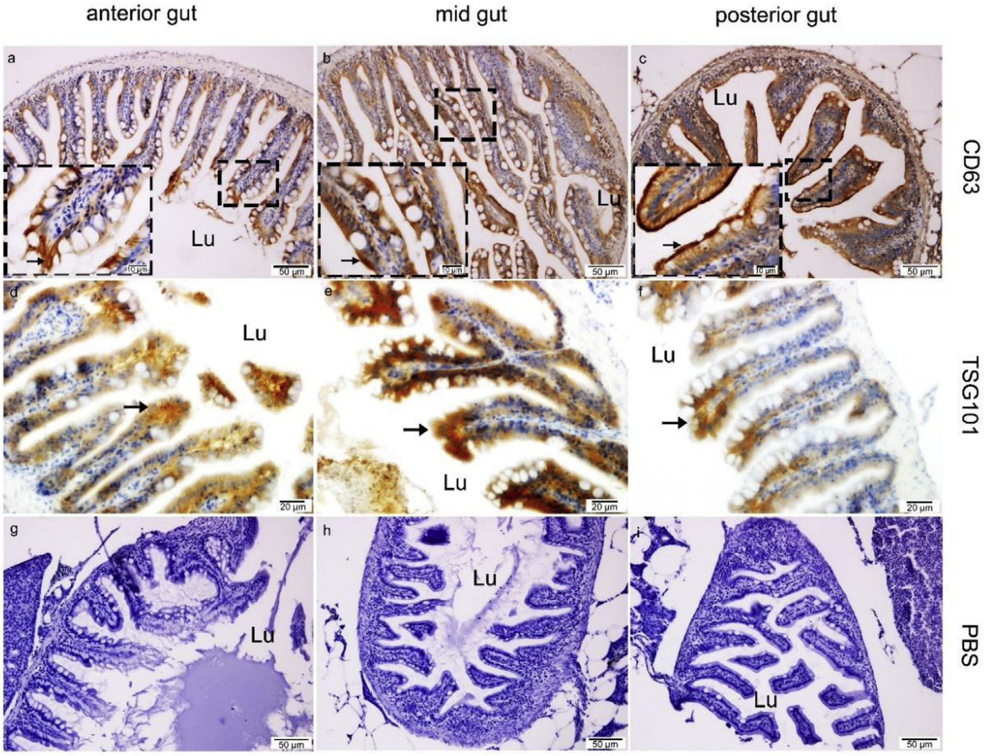

Fig. 2. Immunohistochemical staining for the strongest expression (arrow) of CD63 and TSG101 in different gut epithelium of zebrafish. (a, d, g) Anterior gut; (b, e, h) Mid gut; (c, f, i) Posterior gut; (g, h, i) Negative control. Lu: Lumen; Positive response (arrow); Bars: (a, b, c, g, h, i) = 50 μm; (d, e, f) = 20 μm.

TSG101; ABclonal Technology, China). Peroxidase-labelled anti-rabbit IgG (1:8000, BS13278, Bioworld Technology Inc, Louis Park, MN) was incubated as the secondary antibody for 45 min at 37 °C. The positive signal was detected by an enhanced chemiluminescence detection system (Vazyme Biotech, China). Differences of the protein expression were analysed using Quantity One software (Bio-Rad, USA). The content of the target proteins is converted into the fold change relative to the average content of the control group.

2.6. Immunohistochemistry (IHC)

To identify MVBs and exosomes of zebrafish gut epithelium, antibodies against CD63 and TSG101 were used. Three different segments of the zebrafish gut were examined. The rabbit anti-CD63 antibody (ab134045, Abcam, Cambridge, UK) was used at a dilution of 1:60, and the rabbit anti-TSG101 antibody (ET1701-59, Huabio, Hangzhou, China) was used at a dilution of 1:100. Sections incubated in PBS alone served as negative controls. Images were taken with a light microscope (DP73, Olympus, Tokyo, Japan).

2.7. Immunofluorescence (IF)

Tissue paraffin sections were incubated with primary anti-CD63 (1: 60, ab134045, Abcam, Cambridge, UK) and with primary anti-TSG101 (1:100, ET1701-59, Huabio, Hangzhou, China) separately. Secondary antibodies, Alexa Fluor 488 donkey anti-goat IgG (H + L) antibody (1:100, Invitrogen), were applied for 60 min at room temperature. Samples were sealed with mounting medium containing DAPI. Images were taken with a BX53 Olympus DP73.

2.8. Transmission electron microscopy (TEM)

For the ultrastructural analysis, three segments of the zebrafish gut were dissected and fixed in 2.5% (v/v) glutaraldehyde in 0.1 M phosphate-buffered saline (PBS; 4 °C, pH 7.4; overnight). Thereafter, they were post-fixed with 1% (w/v) osmium tetroxide in the same buffer for 1 h and washed in buffer. The samples were dehydrated in increasing concentrations of ethanol and infiltrated with a propylene oxide-Araldite mixture for embedding in Araldite. The blocks were sectioned, and ultrathin sections (50 nm) were mounted on Formvar-coated grids, and stained with uranyl acetate and led citrate for 20 min per step. The sections were analysed by TEM (Hitachi H-7650; Japan).

2.9. Statistical analysis

The data were analysed with GraphPad Prism 7.0 software for windows. The results were analysed as the mean with the SEM. The statistical significance of differences was analysed by one-way ANOVA, and statistical analysis was conducted with SPSS 16.0 software (SPSS, Inc, Chicago, IL, USA). The data were significantly different at $P < 0.05$ or $P < 0.01$.

3. Results

3.1. Gross anatomy and morphology of the zebrafish gut

The zebrafish gut forms a typical Z-type appearance with three different segments (Supplementary Fig. S1A) that were discriminated based on morphology: anterior (Supplementary Fig. S1C(a)), mid (Supplementary Fig. S1C(b)) and posterior (Supplementary Fig. S1C(c)) gut. By light microscopy, the gut walls of all three segments were composed of three layers: mucosa, smooth muscle, and serosa (Supplementary Fig. S1C(a, b, c)). There was a significant decrease in the diameter from the anterior to the posterior gut (Supplementary Fig. S1B).

3.2. CD63 and TSG101 in the three segments of the gut: expression in zebrafish mucosa

Using real-time quantitative PCR analysis, the mRNA expression

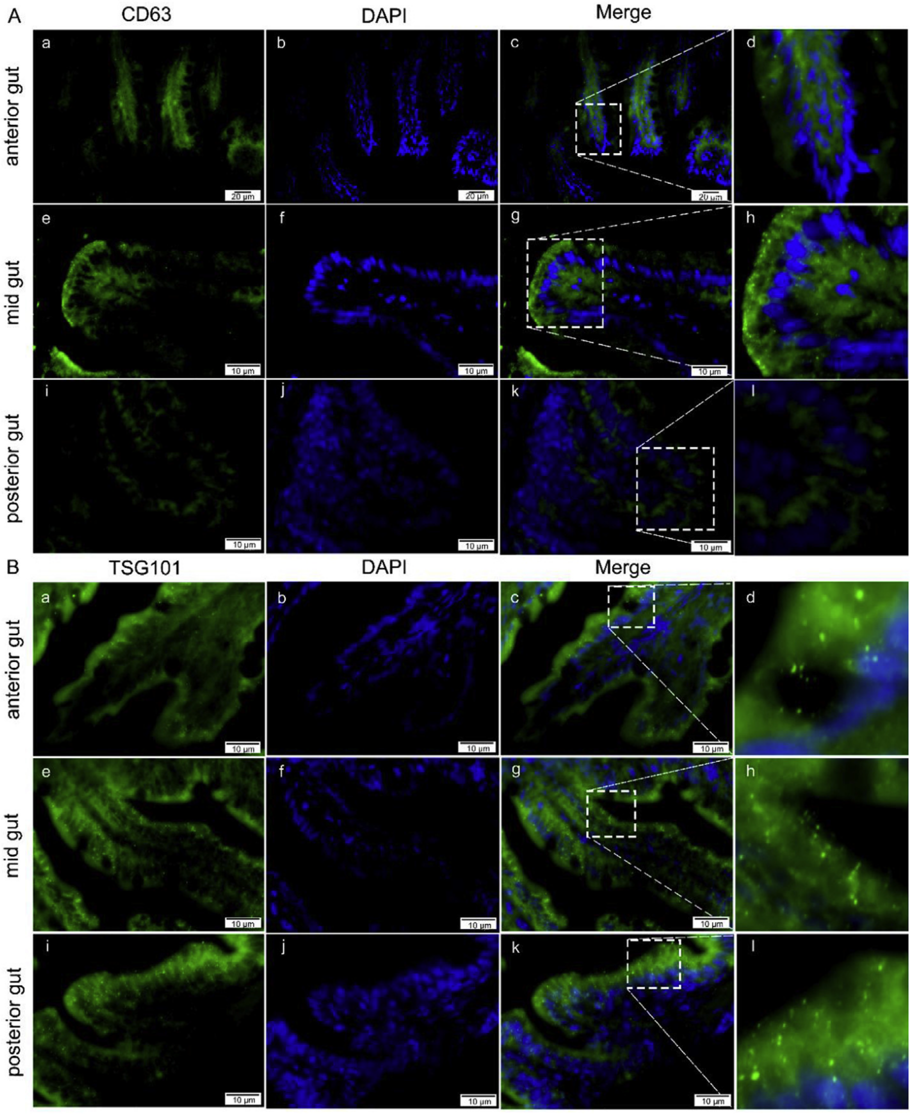

Fig. 3. Immunofluorescent staining of different gut of zebrafish for CD63 and TSG101. (A) CD63 and (B) TSG101 antigen was visualized in anterior gut (a, b, c, d), mid gut (e, f, g, h) and posterior gut (i, j, k, l) by green fluorescence on tissue sections. The blue fluorescence stained nuclei. Bars: A (a, b, c) = 20 μm; A (e, f, g, i, j, k) = 10 μm; B (a, b, c, e, f, g, i, j, k) = 10 μm. (For interpretation of the references to colour in this figure legend, the reader is referred to the Web version of this article.)

level of CD63 was the most significant in the mid gut of zebrafish compared with the posterior gut, followed by the anterior gut. Similarly, the mRNA expression level of TSG101 was the same (Fig. 1A). Moreover, western blotting detected that the expression of CD63 protein in the mid gut was the higher than that in the anterior and the posterior gut. Compared with the anterior and posterior gut, the expression of TSG101 protein was most prominent in the mid gut (Fig. 1B).

To investigate the different expression of critical proteins related to MVBs and exosomes, IHC analysis (Fig. 2)was used to observe the positive reaction of CD63 and TSG101 proteins in the zebrafish gut. In contrast to the negative control sections, the epithelial cell in the different gut showed strong immunoreactivity of CD63 (Fig. 2a, b, c)and TSG101 (Fig. 2d, e, f), especially the apical of gut villi. To future investigate the distribution of MVBs and exosomes in the apical and baselateral cytoplasm of absorptive cells, IF analysis (Fig. 3)was performed to observe the positive structures of CD63 and TSG101 proteins in the absorptive cells. We observed the CD63 strong immunoreactivity particles at the apical cytoplasm of absorptive cells, especially these particles were strongest at the mid gut (Fig. 3A(h)) of zebrafish compared to anterior gut (Fig. 3A(d)) and posterior gut (Fig. 3A(l)). There were many TSG101 positive particles scattered at the apical cytoplasm of absorptive cells of anterior (Fig. 3B(d)), mid (Fig. 3B(h)) and posterior gut (Fig. 3B(l)).

3.3. Ultrastructure of MVBs and their exosomes from absorptive cells in the zebrafish gut (anterior, mid, posterior) by transmission electron microscopy

In the anterior gut epithelium, there were well-arranged columnar-shaped absorptive cells with a brush border (Fig. 4A (a)). Lipid droplets (LDs) were located in the basal cytoplasm of the absorptive cells (Fig. 4A (b)), while early endosomes (ee), late endosomes (le) and multivesicular bodies (MVBs) were difficult to observe in the same regions. Abundant mitochondria (Mit) and single MVB were observed in the apical cytoplasm, and the latter contained several intraluminal vesicles (ILVs) with a diameter of 23.87 ± 4.22 nm (Fig. 4A (c); Table 2).

Compared with the anterior gut, epithelial cells of the posterior gut were irregularly arranged and there were a large number of intraepithelial lymphocytes (Lc) (Fig. 4B (a)). Many pinocytic vesicles

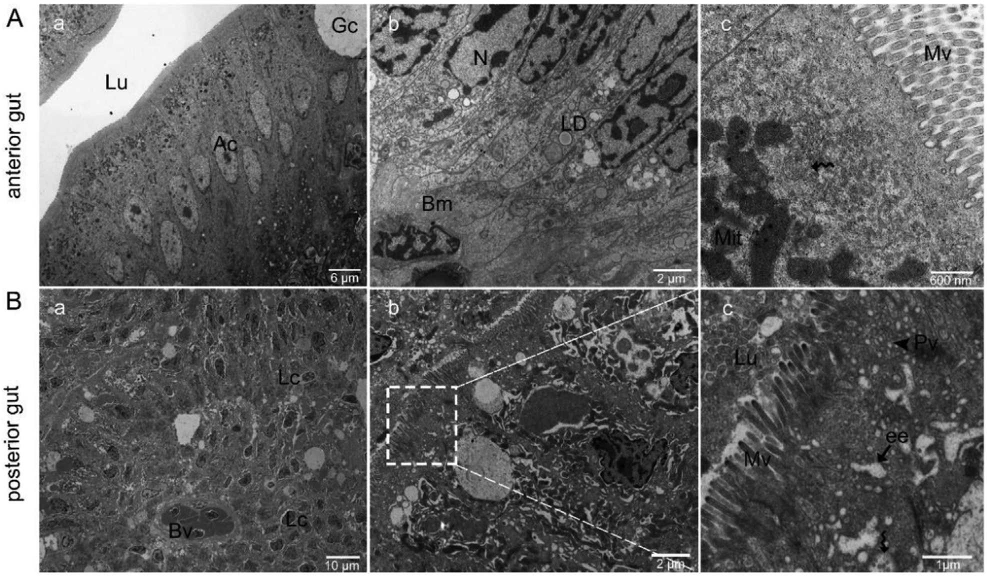

Fig. 4. Localizations of endosomes and MVBs in the anterior and posterior gut of zebrafish by TEM. (A) Anterior gut; (B) Posterior gut; Lu: Lumen; Ac: Absorptive cells; Gc: Goblet cells; Lc: Lymphocytes; Bv: Blood vascular; Mv: Microvilli; LD: Lipid droplet; Bm: Basement membrane; Mit: Mitochondria; MVB: Multivesicular body (Curved arrow); ee: Early endosomes; Pv: Pinocytosis vesicles; N: Nucleus; Bars: A (a = 6 µm; b = 2 µm; c = 600 nm); B (a = 10 µm; b = 2 µm; c = 1 µm).

Table 2

Characteristics of subcellular organelles in the absorptive cells of the different gut of zebrafish (n = 3).

Subcellular organelles	Sizes, Shapes and Locations		
	Anterior gut	Mid gut	Posterior gut
ee	Absent	65.76 ± 33.29 nm Low electron density Basal and apical cytoplasm	Absent
MVB	147.55 ± 5.54 nm Low electron density 23.87 ± 4.22 nm ILVs Apical cytoplasm	177.08 ± 56.14 nm Low electron density 20.03 ± 6.15 nm ILVs Apical cytoplasm; 100.48 ± 21.05 nm High electron density 13.49 ± 3.13 nm ILVs Apical cytoplasm;	51.16 ± 6.24 nm Low electron density Apical cytoplasm
MLB	Absent	156.97 ± 45.38 nm Concentric layers; Dense	Absent
le	Absent	112.07 ± 32.65 nm Low electron density; The inward budding of the Limiting mebrance; Apical cytoplasm	Absent
exo	54 ± 31.07 nm; Mucus layer	61 ± 38.23 nm Mucus layer	46 ± 25.49 nm Deficient
PV	Absent	Absent	Abundant

ee: Early endosomes; MVBs: Multivesicular bodies; MLB: Multilamellar bodies.
le: Late endosomes; Pv: Pinocytosis vesicles; ILVs: Intraluminal vesicles; exo: Exosomes.

existed in the apical cytoplasm of absorptive cells, and MVB and ee were occasionally observed (Fig. 4B (b, c)).

In the mid gut, ee were present at the apical and basal cytoplasm of the absorptive cells (Fig. 5). These ee fused with each other (Fig. 5d). Many Mit were observed surrounded by ee. The ee showed a heterogeneous structure with a diameter of 65.76 ± 33.29 nm. They had low electron density and no ILVs (Table 2). Several multilamellar bodies (MLB) were present in the apical cytoplasm of the same cell (Fig. 5c). Le were distributed in the apical cytoplasm with a small number of ILVs present at the inward budding of the limiting membrane of the le in the absorptive cells (Fig. 5e, f). Unlike the anterior and posterior gut, abundant MVBs were present at the apical cytoplasm in the mid gut absorptive cells (Fig. 5e, f). MVBs, with larger diameters and lower electron densities, were located at the apical area of one absorptive cell (Fig. 5f). Importantly, we observed two distinct morphologies of MVBs with different electron densities. One contained dozens of ILVs with low electron density and a large diameter of 20.03 ± 6.15 nm (Fig. 6a, b; Table 2). The other was relatively small in diameter, with high electron density and ILVs with 13.49 ± 3.13 nm diameter (Fig. 6c, d; Table 2). Therefore, these two MVBs were called "heterogeneous" MVBs. We found several small pits in the roots of microvilli. These pits contained one or more vesicles, and the latter might be the same size as ILVs (Fig. 6e, f), indicating that these vesicles originated from MVBs.

In contrast to the posterior gut (Fig. 7B), many exosomes were mainly distributed in the mucous layer of the anterior (Fig. 7A) and mid (Fig. 7C) gut lumen. The diameter of these exosomes ranged from 30 to 100 nm (Table 2). Interestingly, some MVB-like structures were found in the lumen surrounded by numerous exosomes (Fig. 7C(d)). We summarized all the important features of exosome-associated subcellular organelles in the absorptive cells of the anterior, mid and posterior gut in Table 2.

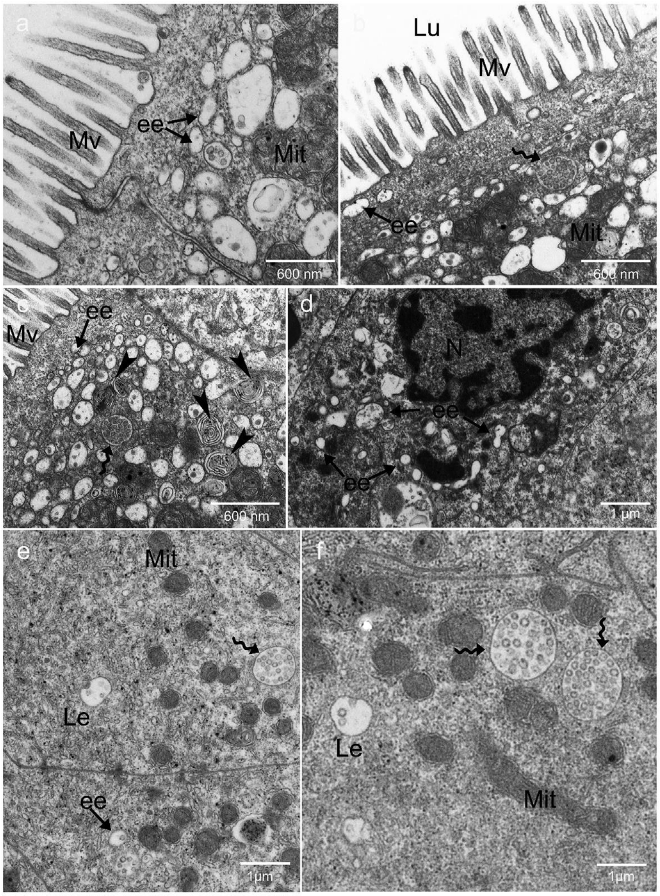

Fig. 5. Characteristics and distribution of early endosomes-late endosomes-MVBs complex in the absorptive cells in the mid gut by TEM. (a, b, c, d) The characteristics of early endosomes in the apical and basal cytoplasm of the absorptive cells. (e, f) The characteristics of late endosomes and MVBs in the apical cytoplasm of the absorptive cells. ee: Early endosomes; Le: Late endosomes; MVB: Multivesicular body (Curved arrow); MLB: Multilamellar body (arrowheads); Mit: Mitochondria; Mv: Microvilli; Lu: Lumen; N: Nucleus; Bars: (a, b, c) = 600 nm; (d, e, f) = 1 µm.

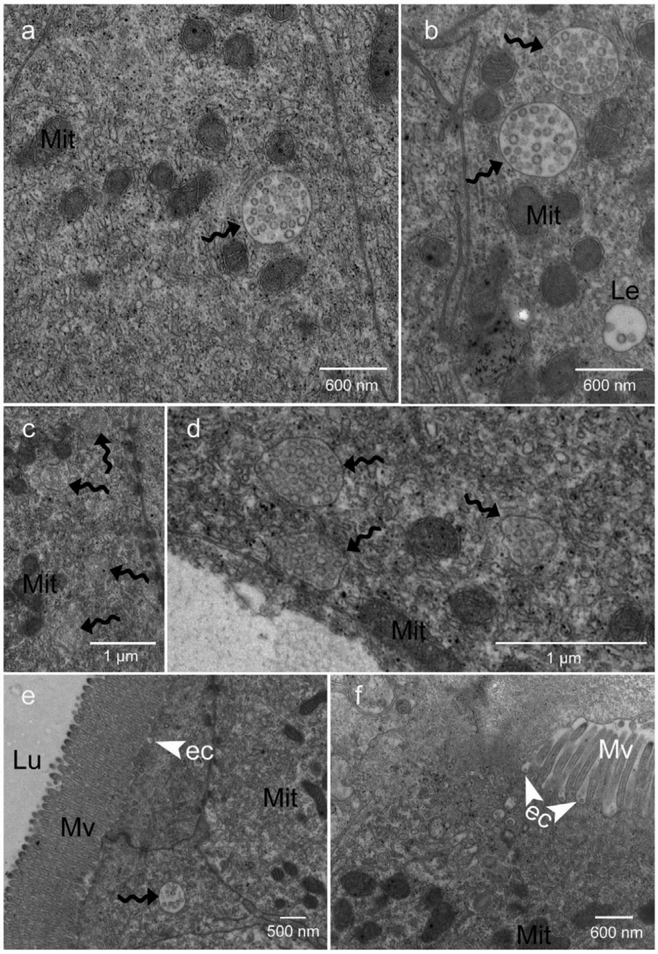

Fig. 6. (a, b, c, d) The characteristics of "heterogeneous" MVBs in the apical cytoplasm of the absorptive cells. (e, f) Exosomes were released via exocytosis at the apical cytoplasm of the absorptive cells in the mid gut. MVB: Multivesicular body (Curved arrow); Le: Late endosomes; Ec: Exocytosis; Mit: Mitochondria; Mv: Microvilli; Lu: Lumen; Bars: (a, b, f) = 600 nm; (c, d) = 1 µm; e = 500 nm.

4. Discussion

The different expression levels of exosome-associated biomarkers in the zebrafish gut were systematically screened and identified by RT-qPCR and WB firstly in this study. The mRNA and protein expression levels of CD63 and TSG101 were the highest in the mid gut among the three segments of the gut. We then detected the distribution of these proteins by IHC and IF. The positive staining of CD63 and TSG101 was observed in the apical cytoplasm of the epithelium in the whole gut, especially in the mid gut. Abundant "heterogenous" MVBs were further analysed by TEM in the mid gut absorptive cells. The endosome-MVB-exosome complex was enriched in the absorptive cells.

The anatomical and histological structure of the zebrafish gut showed similarity with other teleost fish [28,29]. The anterior gut wall with the widest diameter among the three segment. The ultrastructure of the anterior gut showed a small number of MVBs, whereas abundant mitochondria were distributed in the apical cytoplasm of absorptive cells. Many pinocytic vesicles of the posterior gut absorptive cells were observed by TEM. However, there were large numbers of MVBs and their exosomes in the absorptive cells and the lumen of the zebrafish mid gut, which correspond to the small intestine of mammals [30]. At the cellular level, the mid gut epithelial cells of zebrafish might regulate the interaction between the host and the external environment by releasing apical exosomes.

Zebrafish gut epithelial cells must maintain their own homeostasis at all times facing a complex external environment. The principal components of the endocytic pathway consist of early endosomes, late endosomes and lysosomes for mammalian cells [31]. Early endosomes (ee) were widely located in the apical and basal cytoplasm of the mid gut absorptive cells in zebrafish, and fuse with each other as well as being surrounded by a large number of mitochondria. The ee had a diameter of 65.76 ± 33.29 nm, round shape, low electron density, and no intraluminal vesicles (ILVs), which is consistent with the ee of rat ileum epithelial cells [11,12] and baby hamster kidney (BHK-21) cells [32]. Previous studies have shown that once the membrane proteins are endocytosed into the ee, then they are transported to the cell membrane through the circulating endosomes (ce) to maintain the stability of the membrane proteins. Meanwhile, the cytosolic components are endocytosed into another group of ee and then mature into late endosomes (le) [33]. In the present work, le were mainly located under the terminal web of the absorptive cells, with characteristic inward budding of the limiting membrane. Several ILVs within le in zebrafish were observed at the cellular level. The multivesicular late endosomes (MVLE) from human ileal intestinal epithelial cells (IECs) has an important antigen sorting function, and can further secrete basal exosomes which are endocytosed by dendritic cells of the lamina propria to regulate intestinal immune lymphoid tissues [34]. These were characteristic features of le in zebrafish gut absorptive cells and were

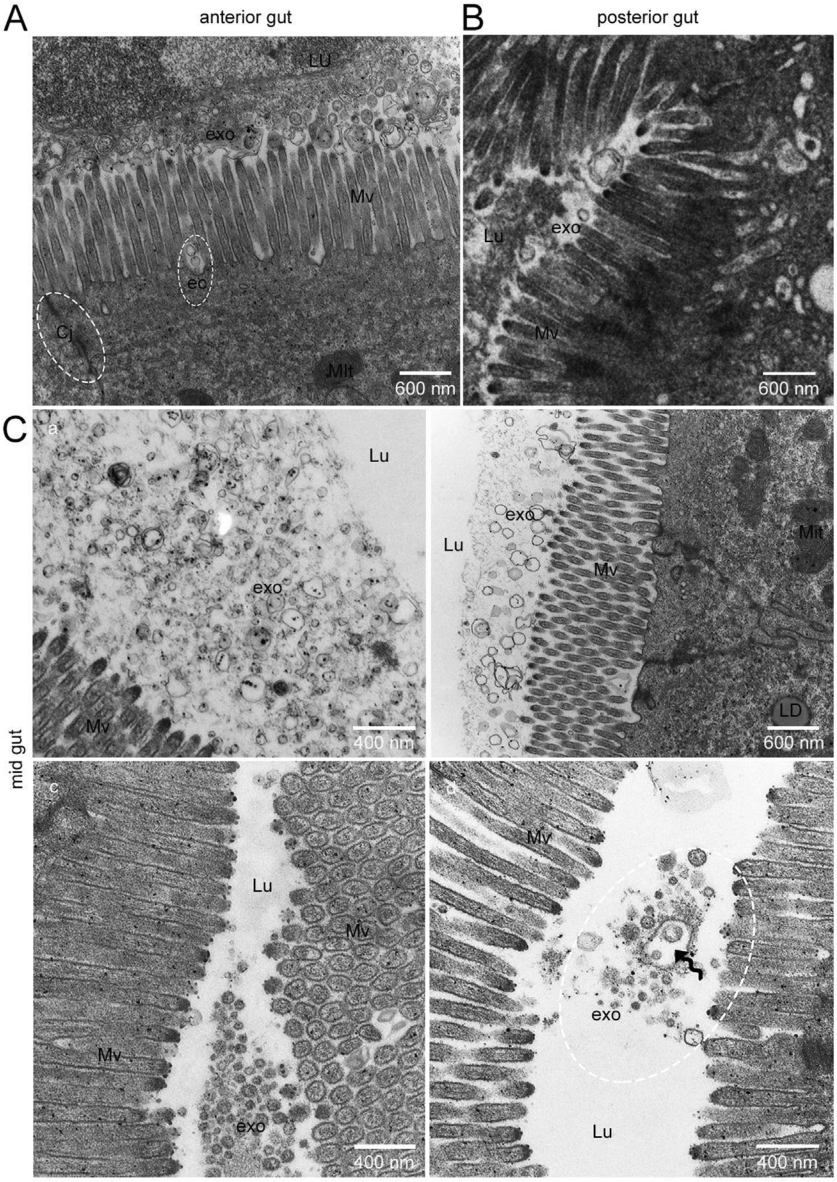

Fig. 7. Distribution of the luminal exosomes in the different segments of gut by TEM. (A) Anterior gut; (B) Posterior gut; (C) Mid gut; exo: Exosomes; MVB-like structure: Multivesicular body-like sturctures (Curved arrow); Mit: Mitochondria; Cj: Cell junction complex; ec: Exocytosis; LD: Lipid droplet; Mv: Microvilli; Lu: Lumen; Bars: A, B = 600 nm; C (a, c, d = 400 nm; b = 600 nm).

morphologically similar to MVLE, suggesting that these cells might have the capacity to adjust gut immune function.

Although scientists have confirmed the formation of le by two different mechanisms based on molecular biology, they have not yet clarified the differences in morphology. In terms of the differences in size, electron density, and number of ILVs, we defined mature le as "heterogenous" MVBs in the zebrafish gut. There are two types of MVBs in mammalian professional antigen presenting cells (APCs), e.g., lymphocyte or dendritic cells, and these MVBs are defined by their expression of major histocompatibility complex (MHC)-II-enriched compartments (MIICs) and exert immune function [35,36]. It was first reported that abundant "heterogenous" MVBs were enriched in the apical cytoplasm of the absorptive cells in this study. Two distinct MVBs were located in the apical cytoplasm of absorptive cells in the mid gut, which had different electron densities, sizes, and locations. MVBs with lower electron density were mainly near the bottom of microvilli, and their diameters varied from 177.08 ± 56.14 nm. MVBs with higher electron density were mostly below them, similar to the "secretive" MVBs and "degradable" MVBs in a mouse oligodendroglial cell line [37–39].

Absorptive cells can exchange substances with the external environment. Exosomes also carry these substances, such as proteins, lipids, metabolites, and virus particles, which act as intermediate information exchanges to maintain gut homeostasis. Previous ultrastructural studies have shown that follicular-associated epithelium (FAE) in sheep have developed transcytosis, including pitting of the luminal membrane, vacuoles, tubular vesicular structures and MVB [40], which is essential for gut mucosal immunity. Similarly, intestinal epithelial cells with typical characteristics similar to FAE are found, although FAE is not existed in the intestinal mucosa of zebrafish, so we speculate that these intestinal epithelial cells also have similar immune functions. Besides, there were many pits in the roots of microvilli and many exosome-like vesicles within these pits in the zebrafish gut epithelium, the exosomes were released from the apical surface into the lumen. Present research has shown that luminal exosomes released from murine intestinal epithelial cell line (IEC4.1)contribute to

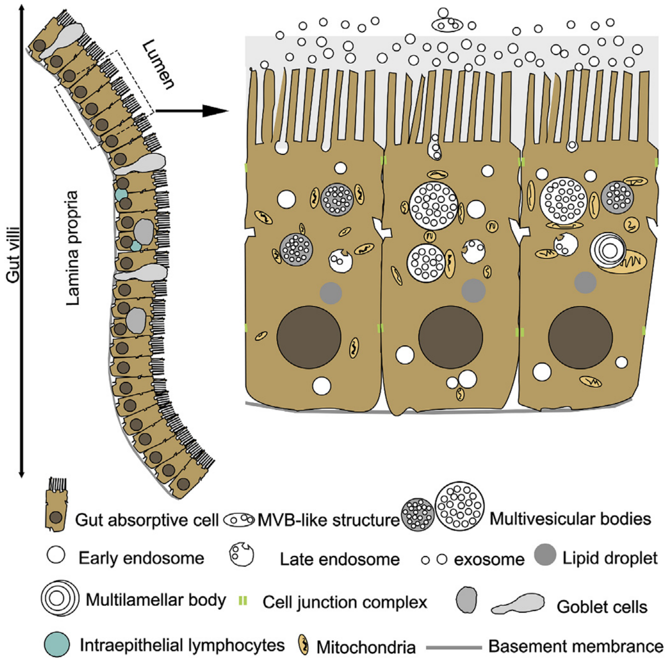

Fig. 8. Schematic diagram of MVBs and their exosomes of the absorptive cells in the mid gut of zebrafish.

epithelial antimicrobial defence, hence we assume that zebrafish gut epithelium may have the similar function in immunity. In the past three decades, studies have shown that the biogenesis of the endocytic pathway is closely related to the differentiation of rat intestinal absorptive cells [12]. As described in rat absorptive cells, we showed that the endosome-MVB-exosome complex was predominantly detected in the absorptive cells along the villus axis. Given the limitations of in vitro cell culture, there is an urgent demand to discover a valuable animal model to elaborate how the in vivo gut epithelial cells release exosomes. Zebrafish could be an ideal animal model for investigating the MVBs and their exosomes from gut, which may provide new insights into human and other animal research in the future.

In conclusion, typical MVBs and their exosomes were differentially distributed, and the endosome-“heterogenous” MVBs-exosome complex was most present in the mid gut absorptive cells. In this study, a schematic diagram of the characteristics and distribution of in vivo gut MVBs and their exosomes was drawn (Fig. 8). In this regard, zebrafish (*Danio Rerio*) may be a valuable animal model for the study of the interaction between exosomes and the gut mucosal immunity. Overall, the characteristics of MVBs and their exosomes in the zebrafish gut provide a potential research platform for the study of exosomes in vivo and contribute to a greater understanding of the subcellular organelles of gut absorptive cells in the future.

Author contributions

Xuebing Bai and Qiusheng Chen conceived and designed the experiments. Xuebing Bai performed most of the experimental task and organized figures. Xuebing Bai and Yanna Guo together drafted the manuscript with assistance and advice from Imran Tarique and Abdul Haseeb. Xindong Wang, Waseem Ali Vistro, Yufei Huang and Hong Chen participated in the study design and performed data analysis. All zebrafish raised by Jinxing Lin. The samples and figures of all zebrafish TEM were completed by Yonghong Shi. Qiusheng Chen, Jinxing Lin and Ping Yang revised the paper. All authors read and approved the final manuscript.

Conflicts of interest

The authors declare no competing financial interests.

Acknowledgments

The authors would like to thank for Xuejing Sun, Taozhi Wang, Enxue Liu and Yu Liang from MOE Joint International Research Laboratory of Animal Health and Food Safety, College of Veterinary Medicine, Nanjing Agricultural University for their excellent technical assistance.

Appendix A. Supplementary data

Supplementary data to this article can be found online at https://doi.org/10.1016/j.fsi.2019.03.030.

Financial support

This research was supported by grants from the National Natural Science Foundation of China (Grant number: 31872433) and Science and Technology Commission of Shanghai Municipality (Grant number: 16140904302).

References

[1] C. Bang, T. Thum, Exosomes: new players in cell-cell communication, Int. J. Biochem. Cell Biol. 44 (11) (2012) 2060–2064.
[2] H. Valadi, K. Ekstrom, A. Bossios, M. Sjostrand, J.J. Lee, J.O. Lotvall, Exosome-mediated transfer of mRNAs and microRNAs is a novel mechanism of genetic exchange between cells, Nat. Cell Biol. 9 (6) (2007) 654–659.
[3] G. van Niel, G. D'Angelo, G. Raposo, Shedding light on the cell biology of extracellular vesicles, Nat. Rev. Mol. Cell Biol. 19 (4) (2018) 213–228.
[4] R.L. Williams, S. Urbe, The emerging shape of the ESCRT machinery, Nat. Rev. Mol. Cell Biol. 8 (5) (2007) 355–368.
[5] M. Babst, G. Odorizzi, E.J. Estepa, et al., Mammalian tumor susceptibility gene 101 (TSG101) and the yeast homologue, Vps23p, both function in late endosomal trafficking, Traffic 1 (3) (2010) 248–258.
[6] A. Doyotte, M.R.G. Russell, C.R. Hopkins, et al., Depletion of TSG101 forms a mammalian `Class E' compartment: a multicisternal early endosome with multiple sorting defects, J. Cell Sci. 118 (Pt 14) (2005) 3003–3017.
[7] M.J. Metzelaar, P.L. Wijngaard, P.J. Peters, et al., CD63 antigen. A novel lysosomal membrane glycoprotein, cloned by a screening procedure for intracellular antigens in eukaryotic cells, J. Biol. Chem. 266 (5) (1991) 3239–3245.
[8] A.C. Theos, S.T. Truschel, D. Tenza, I. Hurbain, D.C. Harper, J.F. Berson, P.C. Thomas, G. Raposo, M.S. Marks, A lumenal domain-dependent pathway for sorting to intralumenal vesicles of multivesicular endosomes involved in organelle morphogenesis, Dev. Cell 10 (3) (2006) 343–354.
[9] M.S. Pols, J. Klumperman, Trafficking and function of the tetraspanin CD63, Exp. Cell Res. 315 (9) (2009) 1584–1592.
[10] G. van Niel, S. Charrin, S. Simoes, M. Romao, L. Rochin, P. Saftig, M.S. Marks, E. Rubinstein, G. Raposo, The tetraspanin CD63 regulates ESCRT-independent and -dependent endosomal sorting during melanogenesis, Dev. Cell 21 (4) (2011) 708–721.
[11] T. Pisitkun, R.F. Shen, M.A. Knepper, Identification and proteomic profiling of exosomes in human urine, P Natl Acad Sci USA 101 (36) (2004) 13368–13373.
[12] G. van Niel, G. Raposo, C. Candalh, M. Boussac, R. Hershberg, N. Cerf-Bensussan, M. Heyman, Intestinal epithelial cells secrete exosome-like vesicles, Gastroenterology 121 (2) (2001) 337–349.
[13] M. Fujita, F. Reinhart, M. Neutra, Convergence of apical and basolateral endocytic pathways at apical late endosomes in absorptive cells of suckling rat ileum invivo, J. Cell Sci. 97 (1990) 385–394.
[14] J.M. Wilson, J.A. Whitney, M.R. Neutra, Biogenesis of the apical endosome-lysosome complex during differentiation of absorptive epithelial cells in rat ileum, Pt 1, J. Cell Sci. 100 (1) (1991) 133–143.
[15] J. Mallegol, G. Van Niel, C. Lebreton, Y. Lepelletier, C. Candalh, C. Dugave, J.K. Heath, G. Raposo, N. Cerf-Bensussan, M. Heyman, T84-intestinal epithelial exosomes bear MHC class II/peptide complexes potentiating antigen presentation by dendritic cells, Gastroenterology 132 (5) (2007) 1866–1876.
[16] M.J. Van N G, C. Bevilacqua, et al., Intestinal epithelial exosomes carry MHC class II peptides able to inform the immune system in mice, Gut 52 (12) (2003) 1690–1697.
[17] B.S. Hong, J.H. Cho, H. Kim, E.J. Choi, S. Rho, J. Kim, J.H. Kim, D.S. Choi, Y.K. Kim, D. Hwang, Y.S. Gho, Colorectal cancer cell-derived microvesicles are enriched in cell cycle-related mRNAs that promote proliferation of endothelial cells, BMC Genomics 10 (2009) 556.
[18] A. Barreto, L.S. Rodriguez, O.L. Rojas, M. Wolf, H.B. Greenberg, M.A. Franco, J. Angel, Membrane vesicles released by intestinal epithelial cells infected with rotavirus inhibit T-cell function, Viral Immunol. 23 (6) (2010) 595–608.

[19] C. Felli, O. Vincentini, M. Silano, A. Masotti, HIV-1 nef signaling in intestinal mucosa epithelium suggests the existence of an active inter-kingdom crosstalk mediated by exosomes, Front. Microbiol. 8 (2017).

[20] G. Hu, A.Y. Gong, A.L. Roth, B.Q. Huang, H.D. Ward, G. Zhu, N.F. Larusso, N.D. Hanson, X.M. Chen, Release of luminal exosomes contributes to TLR4-mediated epithelial antimicrobial defense, PLoS Pathog. 9 (4) (2013) e1003261.

[21] M. Karlsson, S. Lundin, U. Dahlgren, H. Kahu, I. Pettersson, E. Telemo, Tolerosomes" are produced by intestinal epithelial cells, Eur. J. Immunol. 31 (10) (2001) 2892–2900.

[22] E. Dumitrescu, K.N. Wallace, S. Andreescu, Real time electrochemical investigation of the release, distribution and modulation of nitric oxide in the intestine of individual zebrafish embryos, Nitric Oxide: biology and chemistry 74 (2018) 32–38.

[23] S. Brugman, The zebrafish as a model to study intestinal inflammation, Dev. Comp. Immunol. 64 (2016) 82–92.

[24] K.N. Wallace, M. Pack, Unique and conserved aspects of gut development in zebrafish, Dev. Biol. 255 (1) (2003) 12–29.

[25] C. Crosnier, N. Vargesson, S. Gschmeissner, L. Ariza-McNaughton, A. Morrison, J. Lewis, Delta-Notch signalling controls commitment to a secretory fate in the zebrafish intestine, Development 132 (5) (2005) 1093–1104.

[26] A.N. Ng, T.A. de Jong-Curtain, D.J. Mawdsley, S.J. White, J. Shin, B. Appel, P.D. Dong, D.Y. Stainier, J.K. Heath, Formation of the digestive system in zebrafish: III. Intestinal epithelium morphogenesis, Dev. Biol. 286 (1) (2005) 114–135.

[27] K.N. Wallace, S. Akhter, E.M. Smith, K. Lorent, M. Pack, Intestinal growth and differentiation in zebrafish, Mech. Dev. 122 (2) (2005) 157–173.

[28] A. Teles, W.M. Costa, D. Ammar, Y.M. Muller, E.M. Nazari, V.R. Cerqueira, Ontogeny of the digestive tract of Centropomus parallelus larvae, Fish Physiol. Biochem. 41 (2) (2015) 549–559.

[29] M.L. Dos Santos, F.P. Arantes, K.B. Santiago, J.E. Dos Santos, Morphological characteristics of the digestive tract of Schizodon knerii (Steindachner, 1875), (Characiformes: anostomidae): an anatomical, histological and histochemical study, An. Acad. Bras. Cienc. 87 (2) (2015) 867–878.

[30] X.P. Lin, N. Almqvist, E. Telemo, Human small intestinal epithelial cells constitutively express the key elements for antigen processing and the production of exosomes, Blood Cells Mol. Dis. 35 (2) (2005) 122–128.

[31] J. Huotari, A. Helenius, Endosome maturation, EMBO J. 30 (17) (2011) 3481–3500.

[32] J. Gruenberg, Characterization of the early endosome and putative endocytic carrier vesicles in vivo and with an assay of vesicle fusion in vitro, J. Cell Biol. 108 (4) (1989) 1301–1316.

[33] C.T.H. Jonker, R. Galmes, T. Veenendaal, C. Ten Brink, R.E.N. van der Welle, N. Liv, J. de Rooij, A.A. Peden, P. van der Sluijs, C. Margadant, J. Klumperman, Vps3 and Vps8 control integrin trafficking from early to recycling endosomes and regulate integrin-dependent functions, Nat. Commun. 9 (1) (2018) 792.

[34] G. Hundorfean, K.P. Zimmer, S. Strobel, et al., Luminal antigens access late endosomes of intestinal epithelial cells enriched in MHC I and MHC II molecules: in vivo study in Crohn's ileitis, Am. J. Physiol. Gastrointest. Liver Physiol. 293 (4) (2007) G798.

[35] A. Anteunis, Origin and fate of the multivesicular bodies in PHA stimulated lymphocytes, Cell Tissue Res. 149 (4) (1974) 497–511.

[36] L.J. Stern, I. Potolicchio, L. Santambrogio, MHC class II compartment subtypes: structure and function, Curr. Opin. Immunol. 18 (1) (2006) 64–69.

[37] D. Wenzel, A. Schneider, G. Bunt, et al., Neuron to glia signaling triggers myelin membrane exocytosis from endosomal storage sites, JCB (J. Cell Biol.) 172 (6) (2006) 937.

[38] K. Trajkovic, C. Hsu, S. Chiantia, et al., Ceramide triggers budding of exosome vesicles into multivesicular endosomes, Science 319 (5867) (2008) 1244–1247.

[39] S. Mathivanan, J. Hong, R.J. Simpson, Exosomes: extracellular organelles important in intercellular communication, Journal of proteomics 73 (2010) 1907–1920.

[40] C.P. Åkesson, G. Mcgovern, M.P. Dagleish, et al., Exosome-producing follicle associated epithelium is not involved in uptake of PrPd from the gut of sheep (Ovis aries): an ultrastructural study[J], PLoS One 6 (7) (2011) e22180.